The link between reduced porphyry copper deposits and oxidized magmas

Wei-dong Sun [a,*], Hua-ying Liang [a,*], Ming-xing Ling [b], Mei-zhen Zhan [a], Xing Ding [b], Hong Zhang [b,c], Xiao-yong Yang [d], Yi-liang Li [e], Trevor R. Ireland [f], Qi-rong Wei [g], Wei-ming Fan [b]

[a] *Key Laboratory of Mineralogy and Metallogeny, Guangzhou Institute of Geochemistry, Chinese Academy of Sciences, 511 Kehua Street, Wushan, Guangzhou 510640, China*
[b] *State Key Laboratory of Isotope Geochemistry, Guangzhou Institute of Geochemistry, Chinese Academy of Sciences, 511 Kehua Street, Wushan, Guangzhou 510640, China*
[c] *Graduate University of the Chinese Academy of Sciences, Beijing 100049, China*
[d] *Key Laboratory of Crust–Mantle Materials and Environments, University of Science and Technology of China, Hefei 230026, China*
[e] *Department of Earth Sciences, The University of Hong Kong, Pokfulam Road, Hong Kong, China*
[f] *Research School of Earth Sciences, Australian National University, Canberra 0200, Australia*
[g] *China University of Geosciences, Wuhan 430074, China*

Abstract

Porphyry copper deposits account for more than 80% of the world's total Cu resources. However, the formation mechanism and controlling factors of porphyry copper deposits remain obscure. Previous studies have revealed that porphyry copper deposits are usually associated with oxidized, calc-alkalic, adakitic shallow intrusive rocks. Here we show that hematite–magnetite intergrowths are commonly found in porphyry copper deposits, suggesting high and fluctuating oxygen fugacity (fO_2). Oxidation promotes the destruction of sulfides in the magma source, and thereby increases initial chalcophile element concentrations. Sulfide remains undersaturated during the evolution of oxidized sulfur-enriched magmas where sulfate is the dominant sulfur species, leading to high chalcophile element concentrations in evolved magmas. The final porphyry copper mineralization is controlled by sulfate reduction, which starts with magnetite crystallization, accompanied by decreasing pH and correspondingly increasing fO_2. Hematite forms once sulfate reduction lowers the pH sufficiently and the fO_2 reaches the hematite–magnetite oxygen fugacity buffer, which in turn increases the pH for a given fO_2. The oxidation of ferrous iron during the crystallization of magnetite and hematite is the causal process of sulfate reduction and consequent mineralization. Therefore, the initial pH and fO_2 ranges of porphyries favorable for porphyry copper mineralization are defined by the hematite–magnetite oxygen fugacity buffer and SO_4^{2-}–HS^-–S_3^- reaction lines. Adakitic rocks have higher initial contents of copper, sulfur and iron than normal arc rocks, and thus are the best candidates for porphyry copper deposits. These provide a plausible explanation for the formation of copper porphyry deposits. The hematite–magnetite intergrowth marks the upper limits of fO_2 favorable for the mineralization, and thus may be a powerful tool for future prospecting of large porphyry copper deposits.

1. INTRODUCTION

Porphyry Cu–(Au)–(Mo) deposits are one of the most important economic mineral associations (Sillitoe, 1997, 2010; Hedenquist et al., 1998; Heinrich et al., 2004; Cooke

* Corresponding authors.
  E-mail addresses: weidongsun@gig.ac.cn (W. Sun), lianghy@gig.ac.cn (H. Liang).
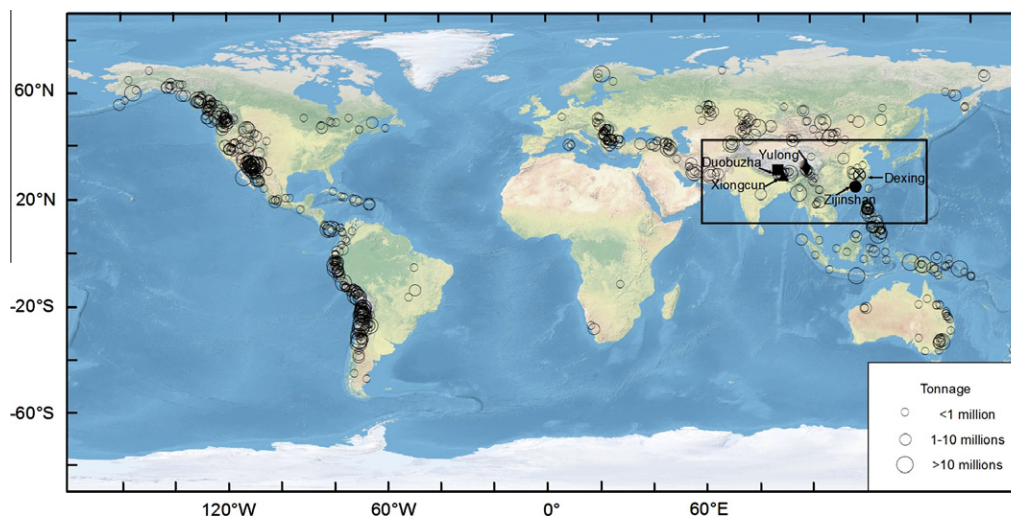
Fig. 1. The distribution of copper porphyry deposits worldwide. More than 90% of the world porphyry copper deposits are located along convergent margins. Data sources: USGS open file (Cooke et al., 2005; Zhang et al., 2006a,b; Liang et al., 2006, 2009; Liu et al., 2010a; Pan and Dong, 1999; USGS, 2011).

et al., 2005), hosting most of the world's copper resources (Ulrich et al., 1999; Halter et al., 2002). More than 90% of the porphyry Cu deposits in the world are distributed along convergent margins (Fig. 1). Porphyry Cu deposits are usually closely associated with a specific type of convergent-margin magma, namely adakite (Sajona and Maury, 1998; Oyarzun et al., 2001; Mungall, 2002), although the association and genetic connections are contentious (Richards and Kerrich, 2007; Sun et al., 2011, 2012b; Richards, 2012). Porphyry Cu deposits are usually closely related to magmas with high oxygen fugacity (fO_2) (Ballard et al., 2002; Sillitoe, 2010), more than two orders of magnitude higher than the fayalite–magnetite–quartz oxygen buffer (ΔFMQ +2) (Mungall, 2002). Nearly all the ore-forming porphyries have abundant sulfate (Liang et al., 2009; Sillitoe, 2010; Xiao et al., 2012). Given that Cu is a chalcophile element, its final mineralization should, however, be mainly controlled by the behavior of reduced sulfur, S^{2-} (Sun et al., 2004; Liang et al., 2009), which inevitably requires the reduction of sulfate (S^{6+}: HSO_4^-/SO_4^{2-}) in the oxidized source magma to sulfides (S^{2-}: H_2S/HS^-/S^{2-}) or polysulfides (e.g., S_2^{2-}, S_3^-) during deposition. The final mineralization of porphyry copper has been attributed to magnetite crystallization (i.e. ferrous iron oxidation) inducing sulfate reduction and corresponding oxygen fugacity fluctuations (Sun et al., 2004; Liang et al., 2009). This is supported by the common occurrence of magnetite in porphyry copper deposits (Vila and Sillitoe, 1991; Mao et al., 2006; Imai et al., 2007b; Khashgerel et al., 2008; Liang et al., 2009; Xu et al., 2009) (Eq. (1)).

$$12Fe^{2+} + SO_4^{2-} + 12H_2O = 4Fe_3O_4 + HS^- + 23H^+ \qquad (1)$$
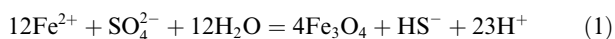
According to Eq. (1), the sulfate reduction and ferrous iron oxidation lead to a decrease of pH in ore-forming fluids within the porphyry system. Consequently, the fO_2 increases because it is controlled by the sulfide–sulfate reaction (Fig. 2) (Pokrovski and Dubrovinsky, 2011). To
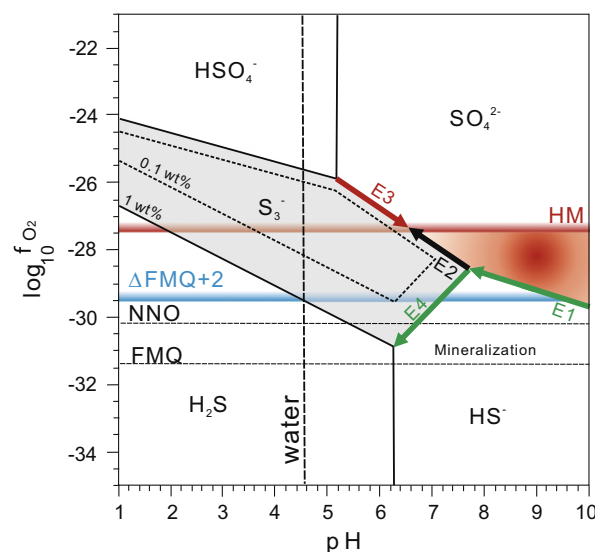

Fig. 2. Stability domains of the trisulfur ion S_3^-, sulfate, and sulfide in an aqueous solution, as a function of oxygen fugacity ($\log_{10} fO_2$, in bars) and acidity (pH = $-\log_{10} m$ H+, in moles per kilogram) at 350 °C and 0.5 GPa illustrating sulfate reduction (modified after (Pokrovski and Dubrovinsky, 2011)). Also shown are the oxygen fugacity of the major mineral buffers (HM, hematite–magnetite; NNO, nickel–nickel oxide; FMQ, fayalite–magnetite–quartz, horizontal dashed lines) and the neutrality point of pure water (the vertical dashed line). The orange field between the hematite–magnetite buffer and SO_4^{2-}–HS^-–S_3^- reaction lines mark the optimal initial oxygen fugacity and acidity of magmas favorable for porphyry copper mineralization. Lines E1, E2, E3, E4, show trajectories for Eqs. 1–4, respectively.

form a porphyry copper deposit with 0.5 wt% of copper in the form of chalcopyrite, the reduction of sulfate and oxidation of ferrous iron results in about 0.36 wt% of H^+ in

the magmas (Eq. 1), which is roughly equivalent to concentrated HCl, assuming 3% of water in the porphyry and assuming there are no pH buffers in the system. Note, ferrous iron is more stable in hydrous solution at lower pH values, such that low pH resulting from sulfate reduction (Eq. 1) hinders the formation of magnetite and HS^-, which is therefore unfavorable for copper porphyry mineralization. In fact, the pH value is usually close to or even higher than neutral values during potassic alteration at the main stage of porphyry copper mineralization. Therefore, the pH value must have been buffered during the mineralization, and thus simple magnetite crystallization alone cannot plausibly drive the formation of porphyry copper deposits.

Here we report magnetite–hematite intergrowths from several large porphyry copper deposits. Although hematite has been reported by many previous authors, little attention has been focused on the intergrowths of hematite and magnetite and their geological significance. This contribution focuses on the chemical reactions that control the mineralization process, and aims to decipher the factors controlling the formation of porphyry copper deposits.

2. BASIC INFORMATION OF STUDIED PORPHYRY DEPOSITS

2.1. Yulong porphyry deposit belt

The Yulong Cu–Mo porphyry deposit belt is located along the eastern margin of the Tibetan Plateau (Yin and Harrison, 2000; Hou et al., 2003; Liang et al., 2007), covering a region about 300 km long and 15–30 km wide. Tectonically, this belt is bounded by a series of strike-slip faults, including the Tuobao-Mankang fault to the west and the Ziga fault and the Gonjo Tertiary basin to the east (Yin and Harrison, 2000; Liang et al., 2007). These deposits are closely associated with Cenozoic high potassium intrusive rocks (Wang et al., 2001; Liang et al., 2007). The porphyries occur as small stocks with surface areas ranging from 0.1 to 0.7 km^2, which intrude Triassic sandstone and limestone, and are characterized by epigenetic features such as explosive breccia (Liang et al., 2006). Five major porphyries, which contain most of the Cu resource in the belt, are located in a narrow, elongated domain approximately 50 km long and 10 km wide that trends in a northwest-southeast direction (Liang et al., 2006). The ore-bearing porphyries typically comprise complex multiphase intrusions, dominated by two major stages. The Yulong porphyry comprises early stage quartz monzonite porphyry and late stage syenogranite porphyry. The Zhanaga porphyry is made up of early stage monzogranite porphyry and late stage syenogranite porphyry. The Mangzong and Duoxiasongduo porphyries, comprise early stage monzogranite porphyry and late stage alkali-feldspar granite porphyry. The Malasongduo porphyry comprises two stages of alkali-feldspar granite porphyry.

The Yulong porphyry is the largest in the copper deposit belt, with >6.5 million tons of copper at an average grade of 0.52% Cu and 0.15 million tons of molybdenum at an average grade of 0.028% Mo. The Zhanaga porphyry hosts more than 0.39 million tons of Cu with a copper content

varying between 0.2% and 0.4%. The Mangzong deposit contains more than 0.3 million tons of Cu at an average grade of 0.3%. The Duoxiasongduo porphyry hosts some 0.45 million tons of copper at an average grade of 0.36%. The Malasongduo porphyry hosts about 1 million tons of Cu with an average grade of 0.35% (Liang et al., 2006, 2009; Hou et al., 2007). The formation ages of the Yulong ore belt ranges from 41.2 to 36.9 Ma, as dated with zircon U–Pb geochronology (Liang et al., 2006).

2.2. Xiongcun porphyry Cu–Au deposit

The Xiongcun (also named as Xietongmen) porphyry Cu–Au deposit is located in the southern rim of the Gangdese orogenic belt in southern Tibet (Tafti et al., 2009; Xu et al., 2009). The Cu–Au mineralization is associated with quartz diorite porphyry, which intrudes the Early Jurassic volcanic sequence (Tafti et al., 2009). It contains more than 130 t of gold with an average grade of 0.61 g/t and more than 1 million tons of Cu metal with an average grade of 0.43%. Main ore minerals include pyrite, chalcopyrite, sphalerite, pyrrhotite, minor galena and molybdenite. Gangue minerals comprise quartz, K-feldspar, andalusite, cordierite, muscovite, biotite, sericite, chlorite, epidote. Veinlet and disseminated mineralization occurs in the quartz diorite porphyry and its adjacent volcanic sequence. Zircon U–Pb ages of the Xiongcun porphyry range from 171.3 ± 1.0 to 173.5 ± 1.0 (2σ) Ma, consistent within error with the molybdenite Re–Os age of 174.2 ± 0.2 Ma (Tafti et al., 2009).

2.3. Duobuza porphyry Cu–Au deposit

The Duobuza porphyry Cu–Au deposit is located at the Bangonhu-Nujinag suture zone situated in the southern margin of the Qiangtang-Sanjiang terrain (Li et al., 2007, 2012). The Duobuza porphyry occurs as small stocks with surface exposures of less than 0.3 km^2 and intrudes the Middle Jurassic siltstone interlayer with andesite, dacite, basalt and chert and Early Cretaceous Meirigie Group volcanic rocks. It contains about 4 million tons of Cu with an average grade of 0.75% and the associated gold content ranges from 0.1 to 1.3 g/t (Li et al., 2008b). Ore minerals comprise chalcopyrite, pyrite, magnetite, bornite, and molybdenite, whereas gangue minerals include K-feldspar, albite, quartz, biotite, sericite, chlorite, calcite and minor anhydrite. Cu–Au mineralization occurs mainly in the potassic alteration zone overprinted by the phyllic or argillization alteration zone (Li et al., 2008b). A SHRIMP U–Pb zircon age of the porphyry (120.9 ± 2.4 Ma) and molybdenite Re–Os isochron age (118.0 ± 1.5 Ma) (Li et al., 2008b) are consistent with each other within uncertainty. It is proposed that the Duobuza porphyry Cu–Au deposit resulted from melt trigged by the northward subduction of Paleo-Tethys oceanic crust (Li et al., 2008b).

2.4. Zijinshan epithermal–porphyry deposit

Zijinshan is the largest Au–polymetallic deposit in southeastern China, with total reserves of Au 320 t, Cu

3 Mt, Mo 0.065 Mt, and Ag 1500 t. It is a complicated epithermal–porphyry mineralization system, consisting of a high-sulfur epithermal Au–Cu deposit, a low-sulfur Ag–polymetallic deposit, and a porphyry Cu–Mo–(Au) deposit. Epithermal deposits are mostly hosted in breccia. The porphyry Cu–Mo–(Au) deposit is hosted in amphibole–biotite- and biotite–granodiorite porphyries with abundant anhydrite indicating oxidizing conditions. Magnetite is abundant in the hornblende biotite granodiorite, which is located under the porphyry Cu–Mo–(Au) deposit.

3. METHODS

Fresh drillhole samples from Yulong, Xiongcun, Duobuza, and Zijinshan porphyry Cu deposits have been studied for this contribution. Special care was taken to avoid secondary hematite formed during sample preparation from magnetite oxidation. Thin sections were first observed using an optical microscope under reflected light immediately after polishing, and then studied with laser Raman spectrometry after repolishing. Raman spectra were recorded with a Renishaw 2000 micro-Raman spectrometer in the backscattering geometry. An argon ion laser emitting at 514.5 nm was used as the excitation source. A thermo-electrically cooled CCD detector was equipped to collect the scattered light dispersed by an 1800 lines/mm grating. All measurements were carried out at room temperature. Raman data were obtained with collection times of about 60 seconds at a power level of 20 mW (Xiao et al., 2007a,b; Tan et al., 2009). The pH-Eh diagram showing the stability domains of the trisulfur ion S_3^-, sulfate, and sulfide in an aqueous solution at 350 °C and 0.5 GPa (Pokrovski and Dubrovinsky, 2011) was used to illustrate the controlling factors during the final mineralization of porphyry Cu deposits.

4. HEMATITE–MAGNETITE AND fO$_2$

Hematite–magnetite intergrowths were found in/near potassic alteration zones from all the porphyry copper deposits studied here, i.e., Yulong porphyry copper–molybdenum–gold deposit belt (Fig. 3) along the eastern margin of the Tibetan plateau, Xiongcun porphyry Cu–Au deposit and Duobuza porphyry Cu–Au deposit on the Tibetan plateau, and Zijinshan Au–Cu–Mo porphyry deposit in Fujian Province (Fig. 4).

Hematite has been reported previously as an accessory mineral in a variety of porphyry copper deposits all over the world, e.g., South America (Vila and Sillitoe, 1991; Patricio and Gonzalo, 2001; Ballard et al., 2002), Southwest Pacific islands (Hedenquist et al., 1998; Imai et al., 2007a), and Mongolia (Khashgerel et al., 2008). Nevertheless, hematite was either ignored or considered a secondary phase, e.g., formed by exsolution (Ballard et al., 2002), or through post mineralization oxidation (Patricio and Gonzalo, 2001). Most of the previously reported hematite in porphyry deposits, however, also appears to be primary and formed before/during the main ore genesis stage. Post-mineralization oxidation cannot explain the coexistence of magnetite–hematite intergrowths and chalcopyrite, e.g.,

Tongshankou porphyry skarn deposit, central eastern China (Li et al., 2008a). Although the oxygen fugacity of fluid inclusions may increase because of diffusional loss of H$_2$ (Mavrogenes and Bodnar, 1994), likely produced through the breakdown of water ($2H_2O = 2H_2 + O_2$), hematite flakes in high-temperature fluid inclusions, e.g., from the Waisoi porphyry deposit, Fiji (Imai et al., 2007a), are also clearly primary.

Primary hematite in close association with magnetite strongly suggests very high oxygen fugacity during porphyry copper mineralization, i.e. fO$_2$ up to about four orders of magnitude higher than the fayalite–magnetite–quartz oxygen buffer (ΔFMQ +4), and about two orders of magnitude higher than the previously recognized lower limit of copper porphyries (Mungall, 2002) (Fig. 2). This then marks the upper fO$_2$ limit for the mineralization. Ferrous iron oxidation is the key link between reduced porphyry copper deposits and oxidized magmas. We argue that the hematite–magnetite buffer is of critical importance to the reduction of sulfate to sulfide and thus porphyry Cu mineralization.

Sulfur is one of the most important elements that can form geosolvents that control the behavior of copper and other chalcophile elements. Therefore it is essential in understanding the mineralization processes of copper and a variety of other metal resources. Recent high-pressure experimental studies show that the trisulfur S_3^- radical ion is an important sulfur species at high-pressure and high-temperature conditions (Fig. 2) (Pokrovski and Dubrovinsky, 2011), which are common for porphyry systems (Hedenquist and Lowenstern, 1994; Seo et al., 2009; Sillitoe, 2010). This requires reevaluation of related geological processes where sulfur is involved, and in particular, porphyry copper mineralization (Pokrovski and Dubrovinsky, 2011).

In contrast to oxygen fugacity buffers, such as HM, FMQ, etc., the oxygen fugacity required for the reduction of sulfate depends strongly on pH. As shown in Fig. 2, in an aqueous solution at 350 °C and 0.5 GPa, as an example, magnetite forms during the reduction of sulfate to HS$^-$ at high pH values and low oxygen fugacity above the FMQ +2 (Eq. 1), whereas either magnetite or hematite forms during the reduction of SO_4^{2-} to S_3^-, depending on the pH values (Eqs. 2 and 3). Nevertheless, magnetite crystallization lowers the pH and increases oxygen fugacity required for sulfate reduction (Fig. 2, Eqs. 1 and 2)

$$6SO_4^{2-} + 52H_2O + 57Fe^{2+} = 2S_3^- + 19Fe_3O_4 + 104H^+ \quad (2)$$
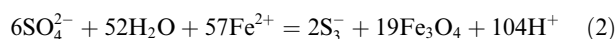
The oxidation potential of the SO_4^{2-}–S_3^- reaction rises with decreasing pH and may reach the hematite–magnetite buffer (Fig. 2), depending on the availability of SO_4^{2-}. For large porphyry deposits, magnetite is further oxidized to hematite by SO_4^{2-}, releasing OH$^-$ (Eq. 3), and in turn increases the pH values. Consequently, the oxygen fugacity of the SO_4^{2-}–S_3^- reaction decreases due to hematite crystallization, which then promotes magnetite formation (Fig. 2). Therefore, magnetite and hematite may grow alternately, which buffers the oxygen fugacity (near the hematite–magnetite buffer) and pH values near neutral (~6–8
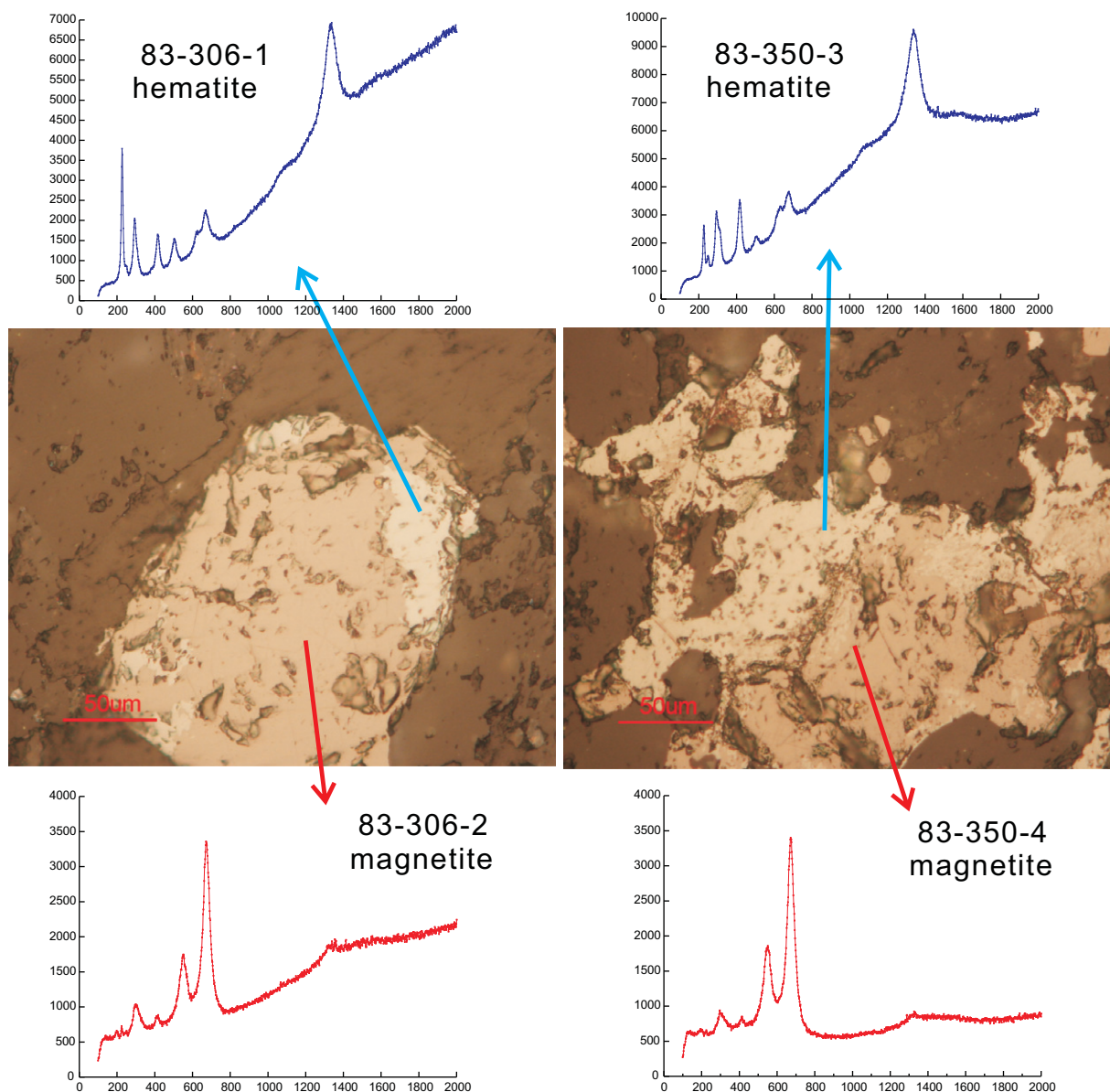
Fig. 3. Reflected light microphotographs and Raman spectra of hematite and magnetite intergrowths from potassic alteration zones of the Yulong porphyry copper belt, along the eastern margin of the Tibetan plateau. Both hematite and magnetite are primary phases. Hematite is usually anhedral, irregularly enclosed in, or intergrown with magnetite, suggesting oscillation in iron oxidation during crystallization.

depending on sulfur concentrations as well as pressure and temperature) during the reduction of SO_4^{2-} to S_3^-.

$$38Fe_3O_4 + 6SO_4^{2-} + 5H_2O = 57Fe_2O_3 + 2S_3^- + 10OH^-$$

$$(3)$$
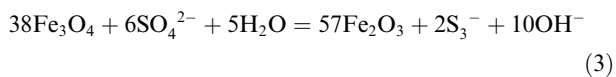
Experimental work shows that the hematite–magnetite redox buffer is the most optimal condition for S_3^- (S_3^- accounts for >50% to 95% of the dissolved sulfur) (Pokrovski and Dubrovinsky, 2011). Compared to reduced sulfur species, SO_4^{2-} has much less influence on the behavior of chalcophile elements (Sun et al., 2004), whereas S_3^- is similar to polysulfide ions like S_3^{2-} and S_2^{2-} that form strong complexes with Au (Berndt et al., 1994) and presumably also

Cu in aqueous solution (Pokrovski and Dubrovinsky, 2011). The formation of S_3^- enhances sulfur mobility in the fluid phase by reducing the amount of sulfur retained in sulfur-bearing minerals (Pokrovski and Dubrovinsky, 2011). Therefore, sulfate reduction (Eqs. 2 and 3) to S_3^- is very important for scavenging copper, gold and other chalcophile elements out of the magma into ore-forming fluids that are of critical importance for the mineralization. For large porphyry deposits, this reduction usually results in the oxidation of magnetite to hematite once the pH value falls (Fig. 2). Therefore, the hematite–magnetite intergrowths may be taken as an indicator assemblage in prospecting future large porphyry copper deposits.
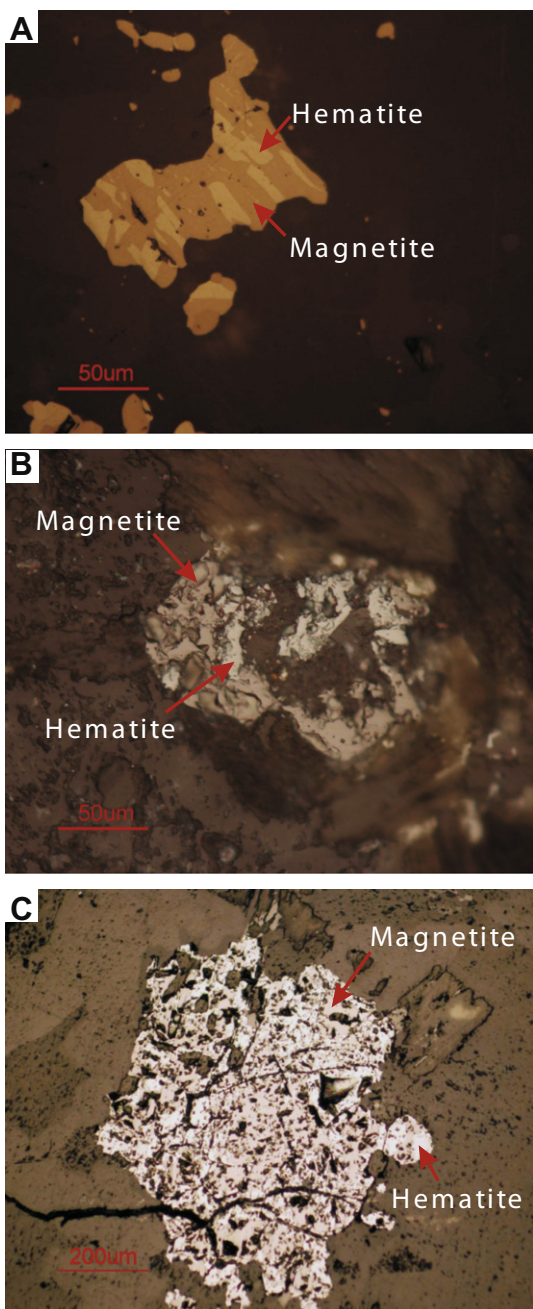
Fig. 4. Examples of reflected light microphotographs of hematite and magnetite intergrowths from potassic alteration zones of the Xiongcun porphyry Cu–Au deposit (A) and Duoboza porphyry Cu–Au deposit on the Tibetan plateau (B), Zijinshan Au–Cu–Mo porphyry deposit in Fujian Province (C). Both hematite and magnetite are primary phases, formed before/during the mineralization process.

5. DISCUSSION

5.1. Sulfur reduction and mineralization

Sulfate is the dominant sulfur species in porphyries associated with large copper deposits (Imai, 2000; Khashgerel et al., 2008; Valencia et al., 2008; Liang et al., 2009; Xiao et al., 2012). Its presence has been cited as the cause of the extraction of additional chalcophile elements from the source region due to the oxidation of sulfide to sulfate during partial melting and the higher solubility of sulfate in silicate liquid (Sun et al., 2004, 2011; Mungall et al., 2006). In contrast, metals of porphyry Cu deposits are hosted in sulfides, which require low oxygen fugacity for stabilization. Elements that can exist in variable oxidation states and that are present in sufficient abundances to affect the redox state of the silicate Earth and silicate magmas include C, H, S, and Fe (Mungall, 2002). In oxidized porphyry magmas, oxidized states, i.e., sulfate, CO_2 and H_2O, are the dominant species, leaving ferrous iron the only reducing agent. Therefore, ferrous iron oxidation during magnetite and hematite crystallization are of critical importance for sulfate reduction and copper mineralization. The optimal initial oxygen fugacity for porphyry copper deposits should be lower than the magnetite–hematite buffer, otherwise there is no ferrous iron in the system. The field between the hematite–magnetite buffer and SO_4^{2-}–HS^-–S_3^- reaction lines (Fig. 2) marks the optimal ranges of pH and oxygen fugacity conditions.

Copper porphyry deposits are also usually associated with calc-alkalic shallow intrusive rocks (Mungall, 2002; Cooke et al., 2005; Sillitoe, 2010). This can be plausibly related to the high pH value of calc-alkalic magmas, which corresponds to a lower oxygen fugacity for the sulfide-sulfate transition line as shown in the pH versus $\log fO_2$ diagram (Fig. 2). Low oxygen fugacity is a favorable condition for copper porphyry mineralization.

The high percentage of S_3^- (>50% to 95% of the dissolved sulfur) and high solubility (up to 1%) of sulfur near the hematite–magnetite redox buffer, coupled with its lower concentration and percentage at oxygen fugacity between nickel–nickel oxide and FMQ buffers with near-neutral pH (Pokrovski and Dubrovinsky, 2011), provide a chemical gradient between the reaction front with high oxygen fugacity close to the hematite–magnetite redox buffer and alteration zones with lower oxygen fugacities farther away. This chemical gradient, in turn, drives S_3^- to the potassic alteration zone, where it further reduces to HS^- and promotes the final mineralization.

In most cases, magnetite crystallizes earlier than hematite, which releases H^+ and consequently increases the oxygen fugacity of sulfate reduction in the system (Fig. 2, Eq. 2), resulting in hematite crystallization and higher pH. H^+ may mobilize potassium from silicate minerals, and trigger potassium alteration. Therefore, the pH value during potassic alteration should be buffered by this reaction to near neutral, near the intersection of the sulfate reduction line and hematite–magnetite buffer (Fig. 2). The potassic alteration zones may be taken as "relay stations" in the building blocks of porphyry copper deposits. This explains the general coincidence of potassic alteration with the ore body.

The final mineralization requires further reduction of S_3^- to S_2^{2-}, HS^-, etc, which also needs the oxidation of ferrous iron to magnetite, further lowering pH values (e.g., Eq. 4). This is probably responsible for triggering sericite alteration at lower pH values.

$$2S_3^- + 20H_2O + 15Fe^{2+} = 6HS^- + 5Fe_3O_4 + 34H^+ \qquad (4)$$

Magnetite formed during this process usually coexists with sulfide. No hematite crystallization is expected. This is supported by the common coexistence of magnetite and sulfide in the sericite alteration zone.

5.2. Adakite and porphyry copper deposits

Adakite was initially proposed to result from partial melting of subducted young oceanic crust (Kay, 1978; Defant and Drummond, 1990). It became a hot topic because of similarities to the Archaean tonalite–trodhjemite–granite (TTG) series (Drummond et al., 1996; Martin, 1999), the importance of such melts to the formation of the continental crust (McDonough, 1991; Rapp et al., 2003; Xiao et al., 2006; Ding et al., 2009; Xiong et al., 2009, 2011), and their close association with large porphyry Cu deposits (Thieblemont et al., 1997; Sajona and Maury, 1998; Oyarzun et al., 2001; Zhang et al., 2004; Sun et al., 2010, 2012a).

Adakite is generally defined on the basis of geochemical compositions (e.g., $SiO_2 \geqslant 56$ wt%, $Al_2O_3 \geqslant 15$ wt%, $Y \leqslant 18$ ppm, $Yb \leqslant 1.9$ ppm and $Sr \geqslant 400$ ppm) (Defant and Drummond, 1990) without detailed petrologic constraints. Therefore, both intrusive and eruptive rocks can be classified as adakites. In addition to the slab melting model (Defant and Drummond, 1990; Yogodzinski and Kelemen, 1998; Martin, 1999; Martin et al., 2005; Moyen, 2009; Liu et al., 2010b), several other mechanisms are proposed for the formation of adakite or adakitic rocks, including (1) partial melting of the lower continental crust (Chung et al., 2003; Gao et al., 2004; Wang et al., 2005), (2) partial meltings of underplated new crust (Petford and Atherton, 1996), and (3) fractional crystallization of normal arc magmas (Castillo, 2006; Macpherson et al., 2006; Richards and Kerrich, 2007).

Most adakites cannot be readily explained by fractionation of normal arc magmas (Sun et al., 2012a). Crystallization of garnet results in higher La/Yb, Sr/Y (Macpherson et al., 2006; Rodriguez et al., 2007) similar to adakites, but this process should also lead to higher and varied Gd/Yb, which is not seen in adakites of a single magma series (Richards and Kerrich, 2007). For this reason, Richards and Kerrich (2007) attributed the adakitic signature to amphibole fractional crystallization. However, this can only increase the Sr/Y in dacite and rhyolite, because Y is highly compatible in felsic magmas, but is incompatible in basaltic andesite and only slightly compatible in andesite (e.g. Bachmann et al., 2005; Xiong, 2006; GERM, 2011). Most adakites are andesitic, and amphibole crystallization cannot increase the Sr/Y ratio quickly enough. More importantly, there is no evidence for pure amphibole crystallization during adakite magma evolution. Plagioclase is a common mineral in arc magmas (e.g., Bachmann et al., 2005; Macpherson et al., 2006), the crystallization of which should considerably decrease Sr concentrations in magmas and erase the adakitic signatures (Sun et al., 2012a).

Some adakitic rocks occur in locations far away from subduction zones or where subduction and collision finished long before magmatism (Zhang et al., 2001; Chung et al., 2003; Wang et al., 2005, 2007a,b; Huang et al., 2008); these have been attributed to partial melting of either thickened (Wang et al., 2007a) or foundered lower continental crust (Gao et al., 2004), or newly underplated mafic crust (Petford and Atherton, 1996; Wen et al., 2008). This kind of "adakite" which can be distinguished from slab melts using isotopic and chemical compositions (Liu et al., 2010b; Ling et al., 2011; Sun et al., 2012a), usually is not associated with Cu porphyry deposits (Sun et al., 2012a).

An increasing number of studies show that most porphyry Cu deposits are closely associated with "true" adakites (Sajona and Maury, 1998; Oyarzun et al., 2001; Gonzalez-Partida et al., 2003; Morozumi, 2003; Reich et al., 2003; Rae et al., 2004; Zhang et al., 2004; Qu et al., 2004b; Borisova et al., 2006; Jiang et al., 2006; Hou et al., 2009; Ling et al., 2009; Sun et al., 2011; Xiao et al., 2012). However, we note that Richards and Kerrich (2007) claimed that adakite-like intrusive rocks are rarely associated with porphyry Cu deposits. This distinction is based on a much more restrictive criteria for adakite that Richards and Kerrich (2007) proposed themselves. For example, Defant and Drummond's (1990) original criterion: "MgO is usually <3% (rarely above 6%)" was changed in Richards and Kerrich (2007) to "MgO <3%, *Mg number ≈ 0.5* (or more correctly 50)". This definition excludes more than 90% of adakites, as defined using the classic criteria such as high Sr and low Y (Sun et al., 2012a). Experiments show that partial melting of MORB with 6.6% MgO produces melts with Mg number lower than 50 (Rapp et al., 1999), i.e., adakites can not be slab melts according to the Richards and Kerrich (2007) criteria. While it is true that slab melts absorb MgO through interaction with mantle peridotite, it is extremely difficult to apply both criteria "Mg number ≈ 50 and MgO contents <3%", because most Cu porphyries have Fe contents higher than 5% (Thompson et al., 1999), which requires MgO contents >5% to fit the Mg number criterion. Several other criteria also act in opposite directions, which "artificially" makes adakites rare under this definition (Sun et al., 2012a).

Richards and Kerrich (2007) also argued that "porphyry Cu deposits are the evolved products of extensive crustal-level processing of calc-alkaline basalt–andesite–dacite–rhyolite series magmas". Porphyry Cu deposits, however, are usually associated with intermediate rocks (Richards, 2011a), which are not highly evolved magmas. Copper is moderately incompatible in most rock-forming minerals, but is compatible in amphibole, such that hornblende crystallization has detrimental effects on Cu mineralization (Sun et al., 2012b). The distribution of copper porphyry deposits along the Pacific subduction zones (Fig. 1) does not support the model of fractional crystallization of hydrous magmas. The subduction of older and wetter oceanic crust in the west Pacific presumably corresponds to magmas more hydrous than those associated with younger and drier oceanic crusts in the east. Nevertheless, there is essentially no known porphyry copper deposit in Japan.

The near absence of porphyry Cu deposits in Archean TTG has been used to argue against the genetic links between adakite and porphyry Cu deposits (Richards and

Kerrich, 2007). However, most TTGs are not porphyritic, probably because only the deeper levels of these granitic plutons are exposed in Archean terranes. At the high pressures at which most TTGs were emplaced, fluids remain dissolved in magmas. Modern porphyry Cu deposits are hosted in shallow intrusive rocks. Lower pressures are essential for fluids to exsolve from magmas during magma evolution (Sun et al., 2007a). Neither hypogene plutons, nor eruptive volcanic rocks, can form porphyry deposits.

The association of adakite with porphyry copper deposits (Thieblemont et al., 1997; Oyarzun et al., 2001; Zhang et al., 2001, 2004; Qu et al., 2004a; Wang et al., 2006a,b, 2007b; Xie et al., 2009) has been attributed to high oxygen fugacity that eliminates sulfides in the mantle source (Mungall, 2002). Most convergent margin magmas, either adakite or normal arc rocks, indicate high oxygen fugacity (Fig. 5) (Ballhaus, 1993; Arculus, 1994; Brandon and Draper, 1996; Parkinson and Arculus, 1999; Kelley and Cottrell, 2009), no matter whether the high oxygen fugacity was primary, resulting from subduction released fluids (Sun et al., 2007b) or secondary, due to higher degrees of magma evolution (Lee et al., 2010). The fact is that porphyry copper deposits are selectively associated with adakitic rocks. Therefore, there must be additional factors that control the association between adakites and porphyry copper deposits.

High oxygen fugacity aside, slab melts have much higher initial copper concentrations than normal arc rocks (Sun et al., 2010, 2011, 2012b), because of the much higher Cu abundances in MORB (Hofmann, 1988; Sun et al., 2003a,b) than in the continental crust (Rudnick and Foun-

tain, 1995; Rudnick and Gao, 2003) and the mantle (McDonough and Sun, 1995). In addition, oceanic crust has sulfur abundances over 1000 ppm (O'Neill and Mavrogenes, 2002), which is about 4 times that of mantle peridotite values (McDonough and Sun, 1995) and more than 2 times the continental crust abundance (Rudnick and Gao, 2003). The solubility of sulfur increases dramatically with increasing oxygen fugacity (Jugo, 2009; Jugo et al., 2010). In case there is residual sulfide, the sulfide concentration in melts is independent of oxygen fugacity, and usually undersaturated during ascent (Mavrogenes and O'Neill, 1999). Additional sulfur is presented in the form of sulfate at high oxygen fugacity. The higher sulfur concentration in oceanic crust (source rocks), together with the high oxygen fugacity of adakite at convergent margins, results in considerably higher sulfate and total sulfur concentrations in slab melts than normal arc rocks at the same oxygen fugacity. This is consistent with the high sulfur contents of several thousand ppm in ore forming porphyries (Xiao et al., 2012). In addition, the iron content of MORB is higher than mantle peridotite, such that slab melt tends to have higher iron contents than mantle derived-magmas. All these factors promote porphyry copper mineralization.

In summary, Cu is a moderately incompatible element with abundances of ~30 ppm in the primitive mantle (McDonough and Sun, 1995), ~26 ppm in the continental crust (Rudnick and Gao, 2003), and roughly the same value for the asthenospheric mantle. Simple magmatic processes cannot raise its concentration by more than 100 times to form Cu porphyry deposits. Moreover, Cu is compatible in amphibole, such that amphibole fractional crystallization has a negative effect on Cu mineralization. Therefore, neither fractional crystallization nor partial melting of the continental crust can explain the close association between adakite and Cu deposits. Slab melts have considerably higher initial Cu, S contents and also high oxygen fugacities, a combination promoting Cu porphyry mineralization (Sun et al., 2011, 2012a).

5.3. Ore-forming conditions and the stability of the trisulfur S_3^- ion

One may argue that most of the porphyries originated at high temperature (i.e., >700 °C) and were then intruded to shallow depths (at pressures lower than 0.5 GPa), conditions which are different from the P–T conditions of Fig. 2. Notwithstanding the lack of low pressure data for the trisulfur S_3^- ion, the P–T conditions chosen in this study are reasonable.

Although ore-forming porphyry magmas formed at high temperature, the final mineralization occurs during the cooling of hydrous magma chambers from >700 °C down to <250 °C (Sillitoe, 2010). The major mineralization likely occurs at temperatures between 400 and 300 °C (Hedenquist et al., 1998; Valencia et al., 2008; Sillitoe, 2010; Richards, 2011b).

The trisulfur S_3^- ion has been demonstrated to be the dominant sulfur species at temperatures between 250–450 °C and 0.5–3.5 GPa, and is more stable at higher temperature (Pokrovski and Dubrovinsky, 2011), i.e., it is
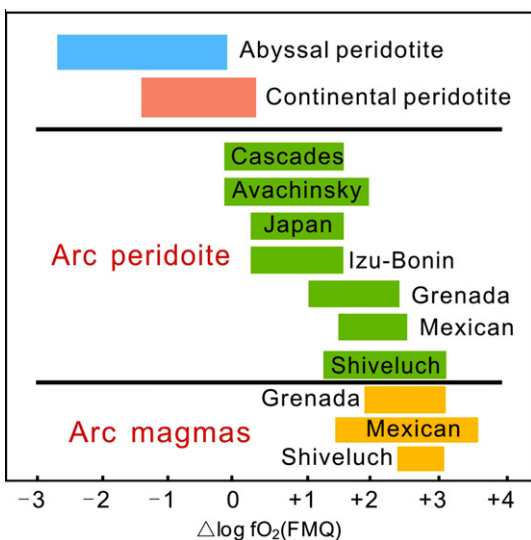

Fig. 5. Oxygen fugacities of major tectonic settings (Bryant et al., 2007). Note that the range of oxygen fugacity for continental peridotite is much smaller than that of (Bryant et al., 2007), after removing peridotite samples from Japan and other arc settings. The oxygen fugacities of convergent margin magmas are systematically higher than those of intraplate settings. Intraplate settings without influence from plate subduction are too reduced for Cu mineralization.

stable at magmatic temperature (Winther et al., 1998). Therefore, our model is also valid at high temperature. Pressure has much less effect on the stability of trisulfur S_3^- ion as illustrated by the available data. It is suggested that trisulfur S_3^- ion is stable and plays a major role at pressures between 0.05 and 0.5 GPa (Pokrovski and Dubrovinsky, 2011). Therefore, the P–T conditions of Fig. 2 are appropriate for illustration.

Most of the porphyries, with the exception of several giant deposits, are small with surface exposure of less than 1 km^2, which is not big enough to supply all the metals locally. Therefore, ore-forming materials must come from additional sources. Studies show that in addition to magmas at shallow depths (at paleodepths < 5 km), porphyry systems are usually related to underlying composite plutons at paleodepths of 5–15 km (Sillitoe, 2010), which supply magmas, fluids and other ore-forming materials for the deposits (Seedorff et al., 2008). The bulk metal budget of porphyry copper deposits is primarily controlled by the composition of the incoming fluid from an underlying magma chamber (Ulrich et al., 1999), therefore, the oscillation of hematite and magnetite crystallizations is probably also common at depths, controlling the supply of metals, sulfur and potassium. This is supported by hematite in drillhole samples from diorite in depths in the Zijinshan porphyry copper deposit.

6. CONCLUSIONS

(1) The final mineralization process of porphyry copper deposits is controlled by the reduction of sulfate at the expense of ferrous iron oxidation. Therefore, the highest initial oxygen fugacity of the magmas favorable for porphyry copper deposits should be lower than the hematite–magnetite buffer, as this provides ferrous iron in the system.

(2) The hematite–magnetite oscillation implies intensive sulfate reduction, which is favorable for giant porphyry copper deposits.

(3) Oxidation of calc-alkalic adakitic rocks with major components from slab melting is one of the best candidates for formation of giant porphyry copper deposits. High oxygen fugacity may eliminate sulfide in the source region and keep the melt sulfide undersaturated, thereby promoting porphyry copper mineralization. Adakitic rocks have higher initial contents of copper, sulfur and iron than normal arc rocks, which are essential for porphyry Cu mineralization.

REFERENCES

Arculus R. J. (1994) Aspects of magma genesis in arcs. *Lithos* **33**, 189–208.

Bachmann O., Dungan M. A. and Bussy F. (2005) Insights into shallow magmatic processes in large silicic magma bodies: the trace element record in the Fish Canyon magma body, Colorado. *Contrib. Miner. Petrol.* **149**, 338–349.

Ballard J. R., Palin J. M. and Campbell I. H. (2002) Relative oxidation states of magmas inferred from Ce(IV)/Ce(III) in zircon: application to porphyry copper deposits of northern Chile. *Contrib. Miner. Petrol.* **144**, 347–364.

Ballhaus C. (1993) Oxidation states of the lithospheric and asthenospheric upper mantle. *Contrib. Miner. Petrol.* **114**, 331–348.

Berndt M. E., Buttram T., Earley D. and Seyfried W. E. (1994) The stability of gold polysulfide complexes in aqueous sulfide solutions – 100 °C to 150 °C and 100 bars. *Geochim. Cosmochim. Acta* **58**, 587–594.

Borisova A. Y., Pichavant M., Polve M., Wiedenbeck M., Freydier R. and Candaudap F. (2006) Trace element geochemistry of the 1991 Mt. Pinatubo silicic melts, Philippines: implications for ore-forming potential of adakitic magmatism. *Geochim. Cosmochim. Acta* **70**, 3702–3716.

Brandon A. D. and Draper D. S. (1996) Constraints on the origin of the oxidation state of mantle overlying subduction zones: an example from Simcoe, Washington, USA. *Geochim. Cosmochim. Acta* **60**, 1739–1749.

Bryant J. A., Yogodzinski G. M. and Churikova T. G. (2007) Melt-mantle interactions beneath the Kamchatka arc: Evidence from ultramafic xenoliths from Shiveluch volcano. *Geochem. Geophys. Geosyst.* **8**, ISI: 000246140400001.

Castillo P. R. (2006) An overview of adakite petrogenesis. *Chin. Sci. Bull.* **51**, 258–268.

Chung S. L., Liu D. Y., Ji J. Q., Chu M. F., Lee H. Y., Wen D. J., Lo C. H., Lee T. Y., Qian Q. and Zhang Q. (2003) Adakites from continental collision zones: Melting of thickened lower crust beneath southern Tibet. *Geology* **31**, 1021–1024.

Cooke D. R., Hollings P. and Walsh J. L. (2005) Giant porphyry deposits: characteristics, distribution, and tectonic controls. *Econ. Geol.* **100**, 801–818.

Defant M. J. and Drummond M. S. (1990) Derivation of some modern arc magmas by melting of young subducted lithosphere. *Nature* **347**, 662–665.

Ding X., Lundstrom C., Huang F., Li J., Zhang Z. M., Sun X. M., Liang J. L. and Sun W. D. (2009) Natural and experimental constraints on formation of the continental crust based on niobium–tantalum fractionation. *Int. Geol. Rev.* **51**, 473–501.

Drummond M. S., Defant M. J. and Kepezhinskas P. K. (1996) Petrogenesis of slab-derived trondhjemite–tonalite–dacite/adakite magmas. *Trans. R. Soc. Edinburgh Earth Sci.* **87**, 205–215.

Gao S., Rudnick R. L., Yuan H. L., Liu X. M., Liu Y. S., Xu W. L., Ling W. L., Ayers J., Wang X. C. and Wang Q. H. (2004) Recycling lower continental crust in the North China craton. *Nature* **432**, 892–897.

GERM, 2011. Geochemical earth reference model. <http://www.earthref.org/GERM/>.

Gonzalez-Partida E., Levresse G., Carrillo-Chavez A., Cheilletz A., Gasquet D. and Solorio-Munguia J. (2003) (Au-Fe) Skarn deposits of the Mezcala district, south-central Mexico: adakite association of the mineralizing fluids. *Int. Geol. Rev.* **45**, 79–93.

Halter W. E., Pettke T. and Heinrich C. A. (2002) The origin of Cu/Au ratios in porphyry-type ore deposits. *Science* **296**, 1844–1846.

Hedenquist J. W., Arribas A. and Reynolds T. J. (1998) Evolution of an intrusion-centered hydrothermal system: far Southeast-Lepanto porphyry and epithermal Cu–Au deposits, Philippines. *Econ. Geol. Bull. Soc. Econ. Geol.* **93**, 373–404.

Hedenquist J. W. and Lowenstern J. B. (1994) The role of magmas in the formation of hydrothermal ore-deposits. *Nature* **370**, 519–527.

Heinrich C. A., Driesner T., Stefansson A. and Seward T. M. (2004) Magmatic vapor contraction and the transport of gold from the porphyry environment to epithermal ore deposits. *Geology* **32**, 761–764.

Hofmann A. W. (1988) Chemical differentiation of the Earth: the relationship between mantle, continental crust, and oceanic crust. *Earth Planet. Sci. Lett.* **90**, 297–314.

Hou Z. Q., Xie Y. L., Xu W. Y., Li Y. Q., Zhu X. K., Khin Z., Beaudoin G., Rui Z. Y., Wei H. A. and Ciren L. (2007) Yulong deposit, eastern Tibet: a high-sulfidation Cu–Au porphyry copper deposit in the eastern Indo-Asian collision zone. *Int. Geol. Rev.* **49**, 235–258.

Hou Z. Q., Yang Z. M., Qu X. M., Meng X. J., Li Z. Q., Beaudoin G., Rui Z. Y., Gao Y. F. and Zaw K. (2009) The Miocene Gangdese porphyry copper belt generated during post-collisional extension in the Tibetan Orogen. *Ore Geol. Rev.* **36**, 25–51.

Hou Z. Q., Zaw K., Pan G. T., Xu Q., Li X. Z., Mo X. X. and Hu Y. Z. (2003) Tectonic setting, metallogenesis and deposit types in Sanjiang Tethyan domain, SW China. *Miner. Explor. Sustain. Dev.* **1–2**, 1165–1168.

Huang F., Li S. G., Dong F., He Y. S. and Chen F. K. (2008) High-Mg adakitic rocks in the Dabie orogen, central China: implications for foundering mechanism of lower continental crust. *Chem. Geol.* **255**, 1–13.

Imai A. (2000) Mineral paragenesis, fluid inclusions and sulfur isotope systematics of the Lepanto Far Southeast porphyry Cu–Au deposit, Mankayan, Philippines. *Resour. Geol.* **50**, 151–168.

Imai A., Ohbuchi Y., Tanaka T., Morita S. and Yasunaga K. (2007a) Characteristics of porphyry Cu mineralization at Waisoi (Namosi district), Viti Levu, Fiji. *Resour. Geol.* **57**, 374–385.

Imai A., Shinomiya J., Soe M. T., Setijadji L. D., Watanabe K. and Warmada I. W. (2007b) Porphyry-type mineralization at Selogiri area, Wonogiri regency, Central Java, Indonesia. *Resour. Geol.* **57**, 230–240.

Jiang Y. H., Jiang S. Y., Ling H. F. and Dai B. Z. (2006) Low-degree melting of a metasomatized lithospheric mantle for the origin of Cenozoic Yulong monzogranite-porphyry, east Tibet: geochemical and Sr–Nd–Pb–Hf isotopic constraints. *Earth Planet. Sci. Lett.* **241**, 617–633.

Jugo P. J. (2009) Sulfur content at sulfide saturation in oxidized magmas. *Geology* **37**, 415–418.

Jugo P. J., Wilke M. and Botcharnikov R. E. (2010) Sulfur K-edge XANES analysis of natural and synthetic basaltic glasses: implications for S speciation and S content as function of oxygen fugacity. *Geochim. Cosmochim. Acta* **74**, 5926–5938.

Kay R. W. (1978) Aleutian magnesian andesite: melts from subducted Pacific Ocean crust. *J. Volcanol. Geoth. Res.* **4**, 117–132.

Kelley K. A. and Cottrell E. (2009) Water and the oxidation state of subduction zone magmas. *Science* **325**, 605–607.

Khashgerel B. E., Kavalieris I. and Hayashi K. (2008) Mineralogy, textures, and whole-rock geochemistry of advanced argillic alteration: Hugo Dummett porphyry Cu–Au deposit, Oyu Tolgoi mineral district, Mongolia. *Mineral. Deposita* **43**, 913–932.

Lee C. T. A., Luffi P., Le Roux V., Dasgupta R., Albarede F. and Leeman W. P. (2010) The redox state of arc mantle using Zn/Fe systematics. *Nature* **468**, 681–685.

Li G. M., Li J. X., Qin K. Z., Dou J., Zhang T. P., Xiao B. and Zhao J. X. (2012) Geology and hydrothermal alteration of the Duobuza gold-rich porphyry copper district in the Bangongco metallogenetic belt, northwestern Tibet. *Resour. Geol.* **62**, 99–118.

Li G. M., Li J. X., Qin K. Z., Zhang T. P. and Xiao B. (2007) High temperature salinity and strong oxidation ore-forming fluid at Duobuza gold-rich porphyry copper deposit in the Bangonghu tectonic belt, Tibet: evidence from fluid inclusions. *Acta Petrol. Sin.* **23**, 935–952.

Li J. W., Zhao X. F., Zhou M. F., Vasconcelos P., Ma C. Q., Deng X. D., de Souza Z. S., Zhao Y. X. and Wu G. (2008a) Origin of the Tongshankou porphyry-skarn Cu–Mo deposit, eastern Yangtze craton, Eastern China: geochronological, geochemical, and Sr–Nd–Hf isotopic constraints. *Mineral. Deposita* **43**, 315–336.

Li J. X., Li G. M., Qin K. Z. and Xiao B. (2008b) Geochemistry of porphyries and volcanic rocks and ore-forming geochronology of Duobuza gold-rich porphyry copper deposit in Ban gonghu belt, Tibet: constraints on metallogenic tectonic settings. *Acta Petrol. Sin.* **24**, 531–543.

Liang H. Y., Campbell I. H., Allen C., Sun W. D., Liu C. Q., Yu H. X., Xie Y. W. and Zhang Y. Q. (2006) Zircon Ce^{4+}/Ce^{3+} ratios and ages for Yulong ore-bearing porphyries in eastern Tibet. *Mineral. Deposita* **41**, 152–159.

Liang H. Y., Campbell I. H., Allen C. M., Sun W. D., Yu H. X., Xie Y. W. and Zhang Y. Q. (2007) The age of the potassic alkaline igneous rocks along the Ailao Shan-Red River shear zone: implications for the onset age of left-lateral shearing. *J. Geol.* **115**, 231–242.

Liang H. Y., Sun W. D., Su W. C. and Zartman R. E. (2009) Porphyry copper–gold mineralization at Yulong, China, promoted by decreasing redox potential during magnetite alteration. *Econ. Geol.* **104**, 587–596.

Ling M. X., Wang F. Y., Ding X., Hu Y. H., Zhou J. B., Zartman R. E., Yang X. Y. and Sun W. D. (2009) Cretaceous ridge subduction along the Lower Yangtse River Belt, Eastern China. *Econ. Geol.* **104**, 303–321.

Ling M. X., Wang F. Y., Ding X., Zhou J. B. and Sun W. D. (2011) Different origins of adakites from the Dabie Mountains and the Lower Yangtze River Belt, eastern China: geochemical constraints. *Int. Geol. Rev.* **53**, 727–740.

Liu J. M., Zhao Y., Sun Y. L., Li D. P., Liu J., Chen B. L., Zhang S. H. and Sun W. D. (2010a) Recognition of the latest Permian to Early Triassic Cu–Mo mineralization on the northern margin of the North China block and its geological significance. *Gondwana Res.* **17**, 125–134.

Liu S. A., Li S. G., He Y. S. and Huang F. (2010b) Geochemical contrasts between early Cretaceous ore-bearing and ore-barren high-Mg adakites in central-eastern China: implications for petrogenesis and Cu–Au mineralization. *Geochim. Cosmochim. Acta* **74**, 7160–7178.

Macpherson C. G., Dreher S. T. and Thirlwall M. F. (2006) Adakites without slab melting: high pressure differentiation of island arc magma, Mindanao, the Philippines. *Earth Planet. Sci. Lett.* **243**, 581–593.

Mao J. W., Wang Y. T., Lehmann B., Yu J. J., Du A. D., Mei Y. X., Li Y. F., Zang W. S., Stein H. J. and Zhou T. F. (2006) Molybdenite Re–Os and albite Ar-40/Ar-39 dating of Cu–Au–Mo and magnetite porphyry systems in the Yangtze River valley and metallogenic implications. *Ore Geol. Rev.* **29**, 307–324.

Martin H. (1999) Adakitic magmas: modern analogues of Archaean granitoids. *Lithos* **46**, 411–429.

Martin H., Smithies R. H., Rapp R., Moyen J. F. and Champion D. (2005) An overview of adakite, tonalite–trondhjemite–granodiorite (TTG), and sanukitoid: relationships and some implications for crustal evolution. *Lithos* **79**, 1–24.

Mavrogenes J. A. and Bodnar R. J. (1994) Hydrogen movement into and out of fluid inclusions in quartz – experimental evidence and geologic implications. *Geochim. Cosmochim. Acta* **58**, 141–148.

Mavrogenes J. A. and O'Neill H. S. C. (1999) The relative effects of pressure, temperature and oxygen fugacity on the solubility of sulfide in mafic magmas. *Geochim. Cosmochim. Acta* **63**, 1173–1180.

McDonough W. F. (1991) Partial melting of subducted oceanic-crust and isolation of its residual eclogitic lithology. *Philos. Trans. R. Soc. A* **335**, 407–418.

McDonough W. F. and Sun S. S. (1995) The composition of the Earth. *Chem. Geol.* **120**, 223–253.

Morozumi H. (2003) Geochemical characteristics of granitoids of the Erdenet porphyry copper deposit, Mongolia. *Resour. Geol.* **53**, 311–316.

Moyen J. F. (2009) High Sr/Y and La/Yb ratios: the meaning of the "adakitic signature". *Lithos* **112**, 556–574.

Mungall J. E. (2002) Roasting the mantle: slab melting and the genesis of major Au and Au-rich Cu deposits. *Geology* **30**, 915–918.

Mungall J. E., Hanley J. J., Arndt N. T. and Debecdelievre A. (2006) Evidence from meimechites and other low-degree mantle melts for redox controls on mantle–crust fractionation of platinum-group elements. *Proc. Natl. Acad. Sci. USA* **103**, 12695–12700.

O'Neill H. S. C. and Mavrogenes J. A. (2002) The sulfide capacity and the sulfur content at sulfide saturation of silicate melts at 1400 degrees C and 1 bar. *J. Petrol.* **43**, 1049–1087.

Oyarzun R., Marquez A., Lillo J., Lopez I. and Rivera S. (2001) Giant versus small porphyry copper deposits of Cenozoic age in northern Chile: adakitic versus normal calc-alkaline magmatism. *Mineral. Deposita* **36**, 794–798.

Pan Y. M. and Dong P. (1999) The Lower Changjiang (Yangzi/Yangtze River) metallogenic belt, east central China: intrusion- and wall rock-hosted Cu–Fe–Au, Mo, Zn, Pb, Ag deposits. *Ore Geol. Rev.* **15**, 177–242.

Parkinson I. J. and Arculus R. J. (1999) The redox state of subduction zones: insights from arc-peridotites. *Chem. Geol.* **160**, 409–423.

Patricio C. C. and Gonzalo R. S. (2001) Oxide mineralization at the Radomiro Tomic porphyry copper deposit, Northern Chile. *Econ. Geol.* **96**, 387–400.

Petford N. and Atherton M. (1996) Na-rich partial melts from newly underplated basaltic crust: The Cordillera Blanca Batholith, Peru. *J. Petrol.* **37**, 1491–1521.

Pokrovski G. S. and Dubrovinsky L. S. (2011) The S_3^- ion is stable in geological fluids at elevated temperatures and pressures. *Science* **331**, 1052–1054.

Qu X., Hou Z. and Li Y. (2004a) Melt components derived from a subducted slab in late orogenic ore-bearing porphyries in the Gangdese copper belt, southern Tibetan plateau. *Lithos* **74**, 131–148.

Qu X. M., Hou Z. Q. and Li Y. G. (2004b) Melt components derived from a subducted slab in late orogenic ore-bearing porphyries in the Gangdese copper belt, southern Tibetan plateau. *Lithos* **74**, 131–148.

Rae A. J., Cooke D. R., Phillips D. and Zaide-Delfin M. (2004) The nature of magmatism at Palinpinon geothermal field, Negros Island, Philippines: implications for geothermal activity and regional tectonics. *J. Volcanol. Geoth. Res.* **129**, 321–342.

Rapp R. P., Shimizu N. and Norman M. D. (2003) Growth of early continental crust by partial melting of eclogite. *Nature* **425**, 605–609.

Rapp R. P., Shimizu N., Norman M. D. and Applegate G. S. (1999) Reaction between slab-derived melts and peridotite in the mantle wedge: experimental constraints at 3.8 GPa. *Chem. Geol.* **160**, 335–356.

Reich M., Parada M. A., Palacios C., Dietrich A., Schultz F. and Lehmann B. (2003) Adakite-like signature of Late Miocene intrusions at the Los Pelambres giant porphyry copper deposit in the Andes of central Chile: metallogenic implications. *Mineral. Deposita* **38**, 876–885.

Richards J. P. (2011a) High Sr/Y arc magmas and porphyry Cu +/− Mo +/− Au deposits: just add water. *Econ. Geol.* **106**, 1075–1081.

Richards J. P. (2011b) Magmatic to hydrothermal metal fluxes in convergent and collided margins. *Ore Geol. Rev.* **40**, 1–26.

Richards J. P. (2012) Discussion of Sun et al. (2011): 'The genetic association of adakites and Cu–Au ore deposits'. *Int. Geol. Rev.*, 368–369.

Richards J. P. and Kerrich R. (2007) Adakite-like rocks: their diverse origins and questionable role in metallogenesis. *Econ. Geol.* **102**, 537–576.

Rodriguez C., Selles D., Dungan M., Langmuir C. and Leeman W. (2007) Adakitic dacites formed by intracrustal crystal fractionation of water-rich parent magmas at Nevado de Longav volcano (36.2 degrees S; Andean Southern Volcanic Zone, central Chile). *J. Petrol.* **48**, 2033–2061.

Rudnick R. L. and Fountain D. M. (1995) Nature and composition of the continental crust; a lower crustal perspective. *Rev. Geophys.* **33**, 267–309.

Rudnick R. L. and Gao S. (2003) Composition of the continental crust. In *Treatise on Geochemistry* (eds. D. H. Heinrich and K. K. Turekian). Pergamon, Oxford.

Sajona F. G. and Maury R. C. (1998) Association of adakites with gold and copper mineralization in the Philippines. *C. R. Acad. Sci. Ser. IIA* **326**, 27–34.

Seedorff E., Barton M. D., Stavast W. J. A. and Maher D. J. (2008) Root zones of porphyry systems: extending the porphyry model to depth. *Econ. Geol.* **103**, 939–956.

Seo J. H., Guillong M. and Heinrich C. A. (2009) The role of sulfur in the formation of magmatic-hydrothermal copper–gold deposits. *Earth Planet. Sci. Lett.* **282**, 323–328.

Sillitoe R. H. (1997) Characteristics and controls of the largest porphyry copper–gold and epithermal gold deposits in the circum-Pacific region. *Aust. J. Earth Sci.* **44**, 373–388.

Sillitoe R. H. (2010) Porphyry copper systems. *Econ. Geol.* **105**, 3–41.

Sun W. D., Arculus R. J., Bennett V. C., Eggins S. M. and Binns R. A. (2003a) Evidence for rhenium enrichment in the mantle wedge from submarine arc-like volcanic glasses (Papua New Guinea). *Geology* **31**, 845–848.

Sun W. D., Arculus R. J., Kamenetsky V. S. and Binns R. A. (2004) Release of gold-bearing fluids in convergent margin magmas prompted by magnetite crystallization. *Nature* **431**, 975–978.

Sun W. D., Bennett V. C., Eggins S. M., Arculus R. J. and Perfit M. R. (2003b) Rhenium systematics in submarine MORB and back-arc basin glasses: laser ablation ICP–MS results. *Chem. Geol.* **196**, 259–281.

Sun W. D., Binns R. A., Fan A. C., Kamenetsky V. S., Wysoczanski R., Wei G. J., Hu Y. H. and Arculus R. J. (2007a) Chlorine in submarine volcanic glasses from the eastern Manus basin. *Geochim. Cosmochim. Acta* **71**, 1542–1552.

Sun W. D., Ling M. X., Chung S. L., Ding X., Yang X. Y., Liang H. Y., Fan W. M., Goldfarb R. and Yin Q. Z. (2012a) Geochemical constraints on adakites of different origins and copper mineralization. *J. Geol.* **120**, 105–120.

Sun W. D., Ling M. X., Ding X., Chung S. L., Yang X. Y. and Fan W. M. (2012b) The genetic association of adakites and Cu–Au ore deposits: a reply. *Int. Geol. Rev.* **54**, 370–372.

Sun W. D., Ling M. X., Yang X. Y., Fan W. M., Ding X. and Liang H. Y. (2010) Ridge subduction and porphyry copper–gold mineralization: an overview. *Sci. China Earth Sci.* **53**, 475–484.

Sun W. D., Zhang H., Ling M. X., Ding X., Chung S. L., Zhou J. B., Yang X. Y. and Fan W. M. (2011) The genetic association of adakites and Cu–Au ore deposits. *Int. Geol. Rev.* **53**, 691–703.

Sun X. M., Tang Q., Sun W. D., Xu L., Zhai W., Liang J. L., Liang Y. H., Shen K., Zhang Z. M., Zhou B. and Wang F. Y. (2007b) Monazite, iron oxide and barite exsolutions in apatite aggregates from CCSD drillhole eclogites and their geological implications. *Geochim. Cosmochim. Acta* **71**, 2896–2905.

Tafti R., Mortensen J. K., Lanc J. R., Rebagliati M. and Oliver J. L. (2009) Jurassic U–Pb and Re–Os ages for the newly discovered Xietongmen Cu–Au porphyry district, Tibet, PRC: implications for metallogenic epochs in the south Gangdese belt. *Econ. Geol.* **104**, 127–136.

Tan D. Y., Xiao W. S., Zhou W. G., Song M. S., Xiong X. L. and Chen M. (2009) Raman investigation of BaWO(4)-II phase under hydrostatic pressures up to 148 GPa. *Chin. Phys. Lett.* **26**.

Thieblemont D., Stein G. and Lescuyer J. L. (1997) Epithermal and porphyry deposits: the adakite connection. *C. R. Acad. Sci. Ser. IIA* **325**, 103–109.

Thompson J. F. H., Sillitoe R. H., Baker T., Lang J. R. and Mortensen J. K. (1999) Intrusion related gold deposits associated with tungsten–tin provinces. *Mineral. Deposita* **34**, 323–334.

Ulrich T., Gunther D. and Heinrich C. A. (1999) Gold concentrations of magmatic brines and the metal budget of porphyry copper deposits. *Nature* **399**, 676–679.

USGS, 2011. <http://geopubs.wr.usgs.gov/open-file/of99-556/>.

Valencia V. A., Eastoe C., Ruiz J., Ochoa-Landin L., Gehrels G., Gonzalez-Leon C., Barra F. and Espinoza E. (2008) Hydro-thermal evolution of the porphyry copper deposit at La Caridad, Sonora, Mexico, and the relationship with a neigh-boring high-sulfidation epithermal deposit. *Econ. Geol.* **103**, 473–491.

Vila T. and Sillitoe R. H. (1991) Gold-rich porphyry systems in the Maricunga Belt, Northern Chile. *Econ. Geol. Bull. Soc. Econ. Geol.* **86**, 1238–1260.

Wang J. H., Yin A., Harrison T. M., Grove M., Zhang Y. Q. and Xie G. H. (2001) A tectonic model for Cenozoic igneous activities in the eastern Indo-Asian collision zone. *Earth Planet. Sci. Lett.* **188**, 123–133.

Wang Q., McDermott F., Xu J. F., Bellon H. and Zhu Y. T. (2005) Cenozoic K-rich adakitic volcanic rocks in the Hohxil area, northern Tibet: lower-crustal melting in an intracontinental setting. *Geology* **33**, 465–468.

Wang Q., Wyman D. A., Xu J., Jian P., Zhao Z., Li C., Xu W., Ma J. and He B. (2007a) Early Cretaceous adakitic granites in the Northern Dabie Complex, central China: implications for partial melting and delamination of thickened lower crust. *Geochim. Cosmochim. Acta* **71**, 2609–2636.

Wang Q., Wyman D. A., Xu J. F., Zhao Z. H., Jian P., Xiong X. L., Bao Z. W., Li C. F. and Bai Z. H. (2006a) Petrogenesis of Cretaceous adakitic and shoshonitic igneous rocks in the Luzong area, Anhui Province (eastern China): implications

for geodynamics and Cu–Au mineralization. *Lithos* **89**, 424–446.

Wang Q., Wyman D. A., Xu J. F., Zhao Z. H., Jian P. and Zi F. (2007b) Partial melting of thickened or delaminated lower crust in the middle of eastern China: implications for Cu–Au mineralization. *J. Geol.* **115**, 149–161.

Wang Q., Xu J. F., Jian P., Bao Z. W., Zhao Z. H., Li C. F., Xiong X. L. and Ma J. L. (2006b) Petrogenesis of adakitic porphyries in an extensional tectonic setting, Dexing, South China: implications for the genesis of porphyry copper mineralization. *J. Petrol.* **47**, 119–144.

Wen D. R., Chung S. L., Song B., Iizuka Y., Yang H. J., Ji J. Q., Liu D. Y. and Gallet S. (2008) Late Cretaceous Gangdese intrusions of adakitic geochemical characteristics, SE Tibet: petrogenesis and tectonic implications. *Lithos* **105**, 1–11.

Winther K. T., Watson E. B. and Korenowski G. M. (1998) Magmatic sulfur compounds and sulfur diffusion in albite melt at 1 GPa and 1300–1500 degrees C. *Am. Mineral.* **83**, 1141–1151.

Xiao B., Qin K. Z., Li G. M., Li J. X., Xia D. X., Chen L. and Zhao J. X. (2012) Highly oxidized magma and fluid evolution of Miocene Qulong giant porphyry Cu–Mo deposit, Southern Tibet, China. *Resour. Geol.* **62**, 4–18.

Xiao W. S., Hong Z., Tan D. Y., Weng K. N., Li Y. C., Luo C. J., Jing L. and Xie H. S. (2007a) Raman characterization of rutile phase transitions under high-pressure and high-temperature. *Spectrosc. Spect. Anal.* **27**, 1340–1343.

Xiao W. S., Tan D. Y., Li Y. C. and Liu J. (2007b) The effects of high temperature on the high-pressure behavior of CeO$_2$. *J. Phys.: Condens. Matter* **19**.

Xiao Y. L., Sun W. D., Hoefs J., Simon K., Zhang Z. M., Li S. G. and Hofmann A. W. (2006) Making continental crust through slab melting: constraints from niobium-tantalum fractionation in UHP metamorphic rutile. *Geochim. Cosmochim. Acta* **70**, 4770–4782.

Xie J. C., Yang X. Y., Sun W. D., Du J. G., Xu W., Wu L. B., Wang K. Y. and Du X. W. (2009) Geochronological and geochemical constraints on formation of the Tongling metal deposits, middle Yangtze metallogenic belt, east-central China. *Int. Geol. Rev.* **51**, 388–421.

Xiong X. L. (2006) Trace element evidence for growth of early continental crust by melting of rutile-bearing hydrous eclogite. *Geology* **34**, 945–948.

Xiong X. L., Keppler H., Audetat A., Gudfinnsson G., Sun W. D., Song M. S., Xiao W. S. and Yuan L. (2009) Experimental constraints on rutile saturation during partial melting of metabasalt at the amphibolite to eclogite transition, with applications to TTG genesis. *Am. Mineral.* **94**, 1175–1186.

Xiong X. L., Keppler H., Audetat A., Ni H. W., Sun W. D. and Li Y. A. (2011) Partitioning of Nb and Ta between rutile and felsic melt and the fractionation of Nb/Ta during partial melting of hydrous metabasalt. *Geochim. Cosmochim. Acta* **75**, 1673–1692.

Xu W. Y., Pan F. C., Qu X. M., Hou Z. Q., Yang Z. S., Chen W. S., Yang D. and Cui Y. H. (2009) Xiongcun, Tibet: a telescoped system of veinlet-disseminated Cu (Au) mineralization and late vein-style Au (Ag)-polymetallic mineralization in a continental collision zone. *Ore Geol. Rev.* **36**, 174–193.

Yin A. and Harrison T. M. (2000) Geologic evolution of the Himalayan–Tibetan orogen. *Annu. Rev. Earth Planet. Sci.* **28**, 211–280.

Yogodzinski G. M. and Kelemen P. B. (1998) Slab melting in the Aleutians: implications of an ion probe study of clinopyroxene in primitive adakite and basalt. *Earth Planet. Sci. Lett.* **158**, 53–65.

Zhang L. C., Wan B., Li W. Q. and Tang H. F. (2006a) Geochemistry and tectonic setting of copper-bearing porphyries

on the southern margin of Tuba basin, Xinjiang. *Acta Petrol. Sin.* **22**, 225–235.

Zhang L. C., Xiao W. J., Qin K. Z. and Zhang Q. (2006b) The adakite connection of the Tuwu-Yandong copper porphyry belt, eastern Tianshan, NW China: trace element and Sr–Nd–Pb isotope geochemistry. *Mineral. Deposita* **41**, 188–200.

Zhang Q., Qin K. Z., Wang Y., Zhang F. Q., Liu H. T. and Wang Y. (2004) Study on adakite broadened to challenge the Cu and Au exploration in China. *Acta Petrol. Sin.* **20**, 195–204 (in Chinese with English abstract).

Zhang Q., Wang Y., Qian Q., Yang J. H., Wang Y. L., Zhao T. P. and Guo G. J. (2001) The characteristics and tectonic–metallogenic significances of the adakites in Yanshan period from eastern China. *Acta Petrol. Sin.* **17**, 236–244 (in Chinese with English abstract).

Associate Editor: Peter Ulmer